Translational Oncology
www.transonc.com

Volume 10 Number xx Month 2017 pp. 679–685 679

Contrast-Enhanced CT Density Predicts Response to Sunitinib Therapy in Metastatic Renal Cell Carcinoma Patients

Simon Matoori[*,†,‡], Yeeliang Thian[*], Dow-Mu Koh[*], Aslam Sohaib[*], James Larkin[*], Lisa Pickering[*] and Andreas Gutzeit[*,†,‡,§]

[*]Department of Radiology, Royal Marsden Hospital, Downs Road, Sutton, Surrey SM2 5PT, United Kingdom; [†]Department of Chemistry and Applied Biosciences, ETH Zurich, Vladimir-Prelog-Weg 3, 8093 Zurich, Switzerland; [‡]Clinical Research Group, Hirslanden Clinic St. Anna, St. Anna-Strasse 32, 6006 Luzern, Switzerland; [§]Department of Radiology, Paracelsus Medical University Salzburg, Strubergasse 21, 5020 Salzburg, Austria

Abstract

The first-line therapy in metastatic renal cell carcinoma (mRCC), sunitinib, exhibits an objective response rate of approximately 30%. Therapeutic alternatives such as other tyrosine kinase inhibitors, VEGF inhibitors, or mTOR inhibitors emphasize the clinical need to predict the patient's response to sunitinib therapy before treatment initiation. In this study, we evaluated the prognostic value of pretreatment portal venous phase contrast-enhanced computed tomography (CECT) mean tumor density on overall survival (OS), progression-free survival (PFS), and tumor growth in 63 sunitinib-treated mRCC patients. Higher pretreatment CECT tumor density was associated with longer PFS and OS [hazard ratio (HR) = 0.968, $P = .002$, and HR = 0.956, $P = .001$, respectively], and CECT density was inversely correlated with tumor growth ($P = .010$). Receiver operating characteristic analysis identified two CECT density cut-off values (63.67 HU, sensitivity 0.704, specificity 0.694; and 68.67 HU, sensitivity 0.593, specificity 0.806) which yielded subpopulations with significantly different PFS and OS ($P < .001$). Pretreatment CECT is therefore a promising noninvasive strategy for response prediction in sunitinib-treated mRCC patients, identifying patients who will derive maximum therapeutic benefit.

Translational Oncology (2017) 10, 679–685

Introduction

Kidney cancer is currently the 9th and 14th most common cancer in men and women, respectively, and accounted for 143,000 deaths worldwide in 2012 [1]. Renal cell carcinoma (RCC) accounts for 90% of kidney cancer cases, and its incidence is rising [2]. Due to its nonspecific symptoms, renal cell carcinoma is often incidentally diagnosed in unrelated imaging procedures, and metastases are detected in 20% to 30% of the cases at the time of diagnosis [1].

Current clinical practice guidelines by the European Society of Medical Oncology recommend the tyrosine kinase inhibitor sunitinib as one of the first-line treatments for metastatic RCC (mRCC) patients with good, intermediate, and poor prognosis [3,4]. Sunitinib-treated patients showed significantly longer progression-free survival (PFS) and better quality of life compared to those treated with interferon-alfa [5,6]. However, in light of an objective response rate of only 31% [5], the pretreatment identification of patients with a high chance of benefitting from sunitinib therapy is an unmet clinical need [3,7,8]. Alternative first-line treatments for mRCC patients include other tyrosine kinase inhibitors such as pazopanib and sorafenib, the VEGF-inhibitor bevacizumab (in combination with interferon-alfa), and the mTOR-inhibitor temsirolimus [3,4].

Address all correspondence to: Simon Matoori, Current address: Department of Chemistry and Applied Biosciences, ETH Zurich, Vladimir-Prelog-Weg 3, 8093 Zurich, Switzerland.
E-mail: smatoori@ethz.ch
Received 19 March 2017; Revised 3 June 2017; Accepted 5 June 2017

1936-5233
http://dx.doi.org/10.1016/j.tranon.2017.06.001

Currently, the response to sunitinib treatment is assessed based on the Response Evaluation Criteria in Solid Tumors (RECIST) and (revised) Choi criteria [3,9,10]. However, such assessment can only be applied after several weeks of pharmacological treatment, which potentially leads to a delay in the implementation of the most effective treatment in nonresponders [3]. Furthermore, nonresponsive patients risk a worse disease outcome, sunitinib-induced adverse reactions, and higher treatment costs [3]. In the age of personalized medicine, there is an unmet clinical need for new strategies to predict the therapeutic benefit before treatment initiation in mRCC patients.

Several attempts for response prediction and treatment assessment of antiangiogenic therapies have been undertaken, mostly based on contrast-enhanced computed tomography (CECT), magnetic resonance imaging, and ultrasound [7,11–21]. These imaging techniques visualize the distribution of the contrast agent into the neoplastic tissue, reflecting the vascularization of the tumor [22]. CECT is currently the most clinically relevant technique, as arterial and portal venous phase CECT are embedded in the assessment of treatment response (Choi response criteria and their modifications, RECIST) in mRCC patients receiving sunitinib [9,12,23,24].

A study by Han et al. found an association between arterial phase CECT density before treatment and patient outcome in mRCC patients under antiangiogenic therapy [11]. However, the patient population of this study was small, and two different tyrosine kinase inhibitors (sunitinib and sorafenib) were used [11]. In addition, the investigated contrast enhancement phase, the arterial phase, is more prone to hemodynamic biases and timing errors compared with the portal venous phase [23]. Hence, we aim to investigate the relationship between pretreatment mean CECT tumor density in the portal venous phase and overall survival (OS), PFS, and tumor growth in a large cohort of mRCC patients undergoing sunitinib therapy.

Table 1. Summary of Patient Characteristics

Total number of patients	63
Male	47 (74.6%)
Female	16 (25.4%)
Age (years), mean ± standard deviation	60.7 ± 11.3
Previous nephrectomy	45 (71.4%)
Line of treatment	
First	50 (79.4%)
Second	12 (19.1%)
Third	1 (1.6%)
Start dose	
25 mg	1 (1.6%)
37.5 mg	10 (15.9%)
50 mg	52 (82.6%)
Histology	
Clear cell	43 (68.3%)
Sarcomatoid	1 (1.6%)
Chromophobe	2 (3.2%)
Eosinophile	1 (1.6%)
Papillary	3 (4.8%)
Mucinous	1 (1.6%)
Xp11.2 translocation-type renal cell carcinoma, APSL-TFE3 variant	1 (1.6%)
Mixed subtype	11 (17.5%)
ECOG performance status	
0	27 (42.9%)
1	27 (42.9%)
2	7 (11.1%)
3	2 (3.2%)
Heng risk category	
Favorable risk	6 (9.5%)
Intermediate risk	42 (66.7%)
Poor risk	15 (23.8%)
Lesions	148
Lymph node	57 (35.5%)
Kidney	22 (14.9%)
Liver	15 (10.1%)
Adrenal gland	12 (8.1%)
Pleura	12 (8.1%)
Bone	11 (7.4%)
Intramuscular	7 (4.7%)
Local recurrence	5 (3.4%)
Peritoneum	4 (2.7%)
Pancreas	2 (1.4%)
Spleen	1 (0.7%)
Lesion size (mm), mean ± standard deviation	42.5 ± 30.6

Material and Methods

Patient Population

Institutional review board approval and waiver for informed consent were obtained for this retrospective study. Patients diagnosed with mRCC receiving first-line sunitinib treatment at our institution between October 1, 2008, and March 1, 2013, were selected for analysis. The following inclusion criteria were used: mRCC patients under sunitinib therapy and availability of baseline portal venous phase CECT imaging of the thorax, abdomen, and pelvis carried out within 4 weeks before treatment initiation and following two cycles of treatment for response assessment. The following exclusion criteria were applied: 1) unavailability of baseline or follow-up CECT images, 2) performance of either baseline or follow-up CECT without intravenous contrast enhancement, 3) performance of a nonstandardized or suboptimal CECT (e.g., inadequate scan coverage or enhancement), 4) disease at baseline not measurable, 5) completion of less than two cycles of sunitinib treatment, 6) patients who underwent short cycles of sunitinib as neoadjuvant treatment before surgical intervention rather than as maintenance therapy, and 7) lung lesions because of the risk of air-filled cavitations in responding lung lesions which were associated with skewed attenuation measurements in the literature [10,25,26]. The same cohort was published before, but the scope of the former study significantly differed from this study [23].

CT Image Acquisition

CECT imaging of the abdomen, chest, and pelvis was performed on all patients at baseline and after two cycles of sunitinib treatment on a 16– or 128–detector row scanner (GE Lightspeed 16, GE Healthcare; Somatom Definition Flash, Siemens). Iohexol (300 mg iodine/ml, Omnipaque 300; GE Healthcare) was administered intravenously (2 ml/kg body weight) by a power injector at a flow rate adapted to cannula size (3 and 2 ml/s for 20 and 22 gauge, respectively). Portal venous phase imaging was conducted craniocaudally using bolus tracking in the aorta with a threshold of 100 HU (65- to 70-second delay, 120 kVp; 170-350 mAs; collimation, 0.6

Table 2. Multivariate HRs for Death (OS) and Progression (PFS) Determined Using Multivariate Cox Regression Analysis (n = 63)

Predictor	β	Std. Error	HR	95% CI	P Value
OS					
Pretreatment mean CECT density	−0.045	0.013	0.956	0.931-0.982	**.001**
Heng risk category (Intermediate risk)	−0.798	0.406	0.450	0.203-0.997	**.049**
PFS					
Pretreatment mean CECT density	−0.032	0.011	0.968	0.948-0.989	**.002**
Age ≥ 62 years	−0.846	0.316	0.429	0.231-0.797	**.007**

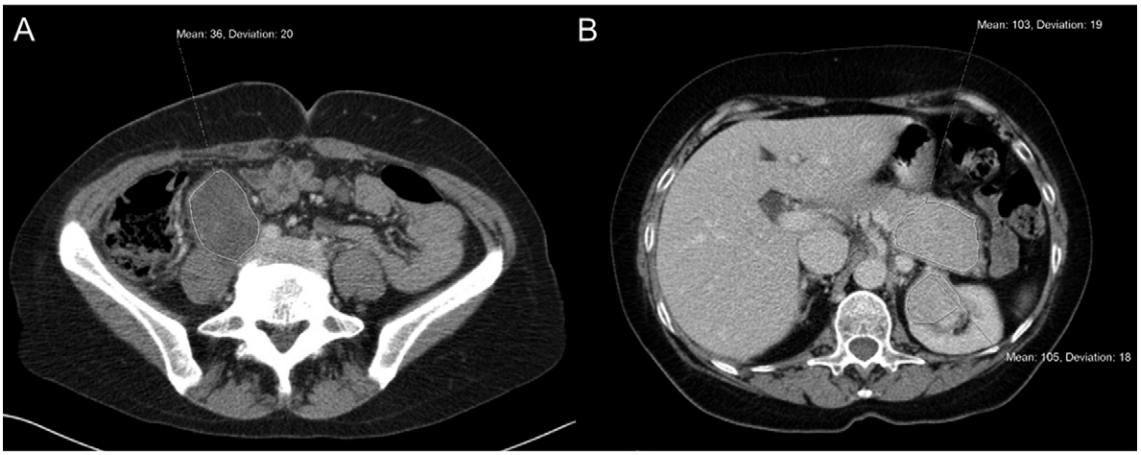

Figure 1. Comparison of a patient with low (A) and a patient with high pretreatment CECT tumor density (B). The female, 49-year-old patient (A) with a low CECT tumor density before treatment initiation had a PFS time of 41 days and an OS time of 59 days. The female, 58-year-old patient (B) with a high pretreatment CECT tumor density in the kidney tumor and a mesenterial metastasis had a PFS time of 420 days and an OS time of 560 days.

mm). Lesion were measured based on data set reconstructions at 5-mm section thickness and 5-mm reconstruction increments.

Image Analysis

Target lesions were defined based on RECIST 1.1 criteria (five target lesions, maximum of two lesions per organ) [27]. Lesions were defined in consensus by two board-certified radiologist with experience in oncological imaging of 13 (A.G.) and 8 years (Y.T.). Unidimensional size and bidimensional attenuation were measured on a single section that represented the largest diameter of each target lesion. The sum of longest dimensions of all lesions was calculated as defined by RECIST 1.1 criteria. The CT attenuation in Hounsfield units of target lesions was determined by drawing a region of interest around the lesion margin on the section selected for size measurement at portal venous phase CT imaging, which gave the mean pixel attenuation for each lesion. This was then averaged for all target lesions to give a mean CT attenuation. The CT attenuation in Hounsfield units of target lesions was determined by two independent readers who drew a region of interest around the lesion on the selected section on portal venous phase CT imaging. The thus obtained mean pixel attenuation was subsequently averaged for all target lesions. This attenuation was again averaged for both readers, yielding a mean CT attenuation. The absolute and relative changes of the sum of tumor diameters and the mean CECT attenuation from the baseline (i.e., before treatment initiation) to the first follow-up were calculated as evidence of tumor growth.

Statistical Analysis

Statistical software (R statistics 3.1.1 and SigmaPlot 13.0) was employed for all statistical analyses. OS and PFS were chosen as the two main outcome measures. OS and PFS were defined as the time span between initiation of sunitinib treatment and death from any cause or censorship at the date of last follow-up (OS) or date of clinically documented tumor progression or death (whichever occurred first) or censorship at the date of last follow-up (PFS). For PFS, progression and death were defined as event. For both outcome parameters, data collection was closed on June 25, 2013. To find the hazard ratios (HRs) of responders to nonresponders for each set of criteria, Cox regression analysis was carried out. First, univariate analyses were performed for patient age, gender, previous nephrectomy, Heng prognostic category (recoded binary: 1 = low and poor risk; 2 = intermediate risk), Eastern Cooperative Oncology Group

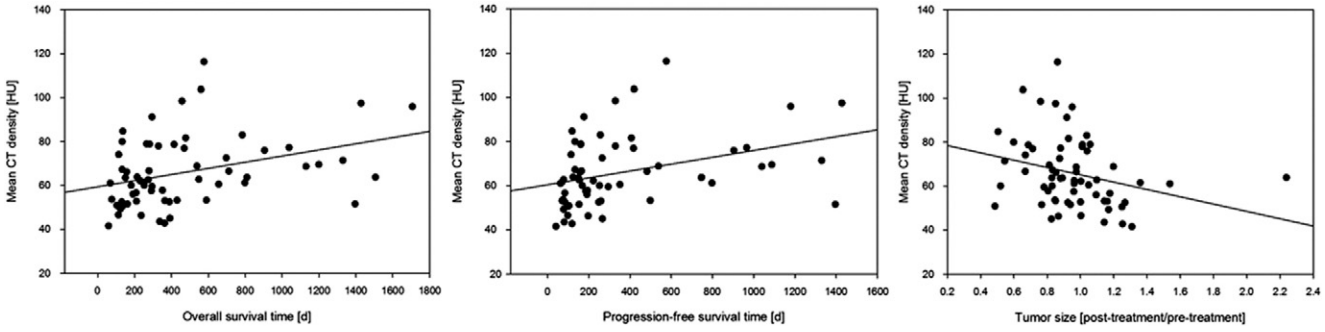

Figure 2. Scatterplots of pretreatment mean CECT tumor density and OS, PFS, and change in tumor size ($n = 63$). Pretreatment mean CECT density shows a positive correlation with OS (Spearman's rho = 0.401, $P = .001$, $n = 63$) and PFS (Spearman's rho = 0.452, $P < .001$, $n = 63$). An inverse correlation was determined for pretreatment mean CECT density and the ratio of tumor size after two treatment cycles (posttreatment) and pretreatment (Spearman's rho = −0.323, $P = .010$, $n = 63$).

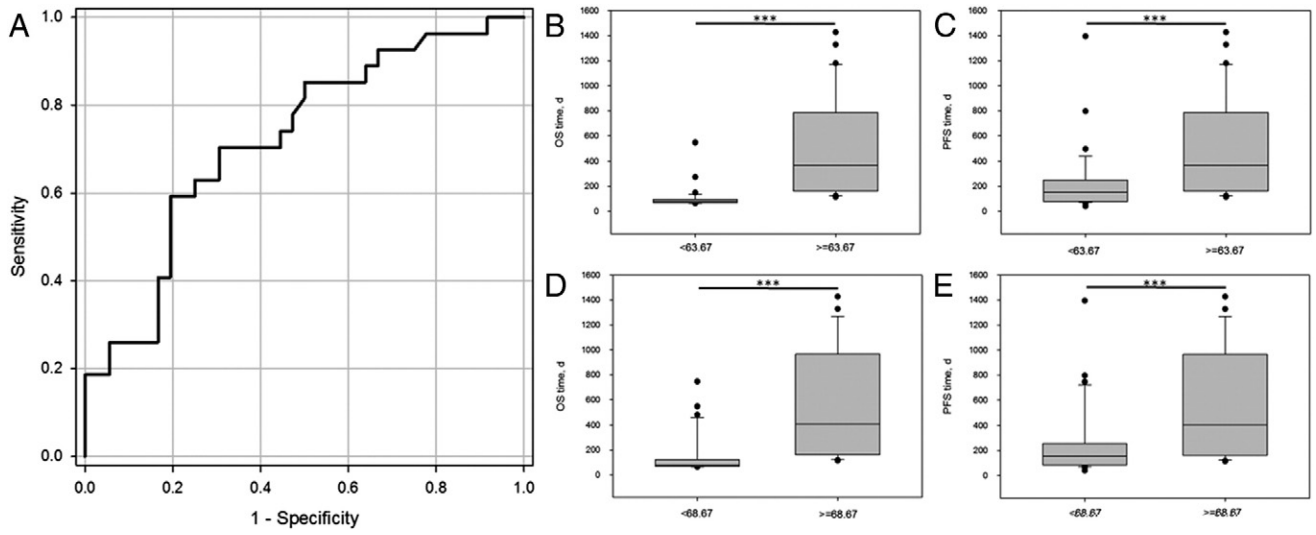

Figure 3. ROC curve based on a PFS time of 250 days and boxplots of the OS and PFS time of subpopulations based on optimal pretreatment mean CECT density cut-off points (n = 63). The ROC curve had an area under the curve of 0.722 (CI 0.595-0.849, P = .003, n = 63, A). A Youden's index analysis yielded two optimal CECT density cut-offs (63.37 HU and 68.67 HU) associated with highly significant differences in OS and PFS (P < .001, n = 63).

(ECOG) performance status (recoded 0; 1; 2-3), aorta CT density, and pretreatment mean CECT density. For categorical variables, the log-rank test of equality across strata was done. For continuous variables, Cox proportional hazard regression was calculated. All predictors that had a P value < .2 in the univariate analyses were considered for the final model of PFS (mean CT density, age, and ECOG performance status) and OS (mean CT density, Heng prognostic category, and ECOG performance status). The assumption of log linearity was checked with linear splines. Age was categorized using the median as cut point. Log minus log survival curves were used to check the proportional hazards assumption. ECOG performance status clearly did not meet this assumption and was therefore used as strata variables in the final model. Spearman's rho was calculated for the correlation between mean CECT tumor density and OS, PFS, and the ratio of tumor size at first follow up divided by tumor size pretreatment. A receiver operating characteristic (ROC) analysis was carried out based on a PFS cut-off of 250 days, and Youden's index was employed to find optimal pretreatment mean CECT tumor density cut-offs (OptimalCutpoints package, R statistics). A nonparametric statistical test (Wilcoxon rank sum test) was employed to investigate differences between the median OS or the median PFS of the subgroups based on these cut-off values. Furthermore, a Kaplan-Meier survival analysis with a log-rank test was conducted. A P value of < .05 was deemed statistically significant.

Results

Baseline Characteristics

Of the 118 patients extracted from the database of our institution, 55 patients were excluded [unavailability of baseline or follow-up CECT images (n = 18), performance of either baseline or follow-up CECT without intravenous contrast enhancement (n = 14), performance of a nonstandardized or suboptimal CECT (e.g., inadequate scan coverage or enhancement) (n = 2), disease at baseline not measurable (n = 7), completion of less than two cycles of sunitinib treatment (n = 3), and patients who underwent short cycles of sunitinib as neoadjuvant treatment before surgical intervention rather than as maintenance therapy (n = 5), patients with lung lesions only (n = 6), and all other lung lesions (15 lesions)]. Thus, 63 patients with 148 lesions were included into the study and eligible for the measurement of the CECT mean tumor density and tumor diameter. The summary of the baseline characteristics of the patient population is presented in Table 1.

Relationship of CECT and Survival

Portal venous phase mean CECT tumor density before treatment was an independent predictor of PFS and OS [HR 0.968, 95% confidence interval (CI) 0.948-0.989, P = .002, and HR 0.956, 95% CI 0.931-0.982, P = .001, respectively; n = 63, number of events = 50; Table 2, Figures 1 and 2, *A* and *B*]. Pretreatment mean CECT density in the portal venous phase was further inversely correlated with tumor growth at first follow-up (Spearman's rho = −0.323, P = .010, Figure 2*C*). Higher pretreatment portal venous phase mean CECT density was therefore significantly associated with prolonged PFS and OS and lower tumor growth at first follow-up (Figure 2).

A ROC analysis of the portal venous phase mean CECT tumor density before treatment using a PFS cut-off of 250 days yielded an area under the curve of 0.722 (standard error 0.065, CI 0.595-0.849, P = .003; PFS < 250 days: 36 patients, PFS > 250 days: 27 patients; Figure 3*A*). Using Youden's index, two optimal mean CT density cut-off points were determined (cut-off 1: 63.67, sensitivity 0.704, specificity 0.694, positive predictive value 0.633, negative predictive value 0.758; cut-off 2: 68.67, sensitivity 0.593, specificity 0.806, positive predictive value 0.696, negative predictive value 0.725). Both cut-offs led to subpopulations with highly significantly different OS and PFS (P < .001, n = 63; Figure 3, *B-E*). Kaplan-Meier survival analysis showed significant differences in the OS and PFS for the subpopulations of both cut-off values (P < .001, n = 63, Figure 4).

Discussion

The main finding of this study is that higher pretreatment portal venous phase mean CECT tumor density was associated with longer

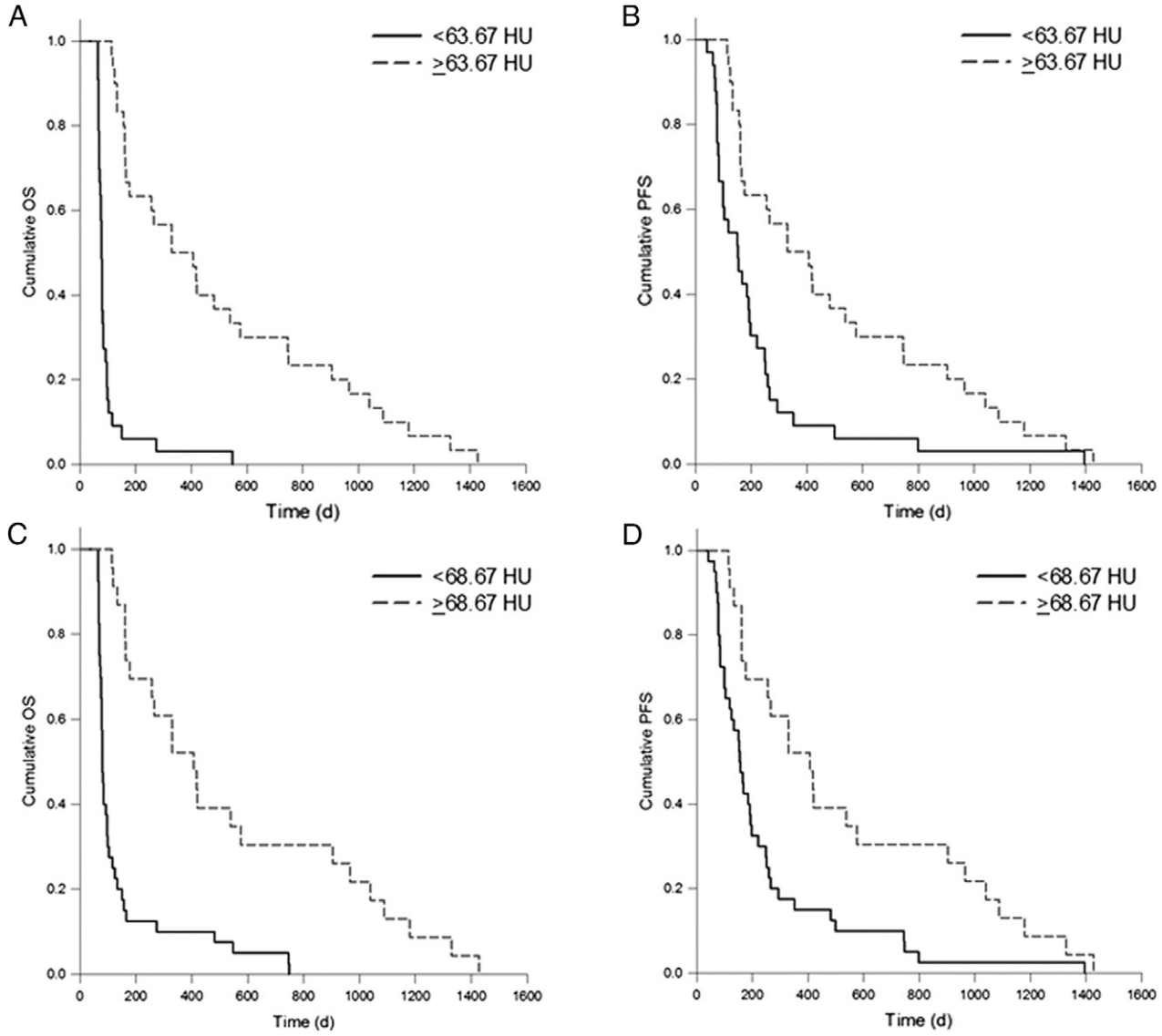

Figure 4. Kaplan-Meier survival curves for pretreatment cut-off 1 (A, B) and cut-off 2 (C, D; $n = 63$). Both cut-offs yield subpopulations with significantly different OS and PFS curves ($P < .001$, $n = 63$) which highlights the usefulness of these two pretreatment mean CECT density cut-off values in subgrouping mRCC patients according to their probability to respond to sunitinib treatment.

PFS and OS in mRCC patients undergoing sunitinib treatment ($P = .002$ and $P = .001$, respectively) and that mean CECT tumor density was inversely correlated with tumor growth after two treatment cycles ($P = .010$). A ROC analysis based on a PFS of 250 days yielded two mean CECT tumor density cut-off values with high sensitivity and specificity which resulted in subpopulations with significantly different survival outcomes ($P < .001$). These findings strongly support the potential predictive value of portal venous phase pretreatment mean CECT tumor density on the patient outcome of mRCC patients receiving sunitinib. Mean CECT tumor density is therefore a promising strategy for treatment stratification and a step toward personalized medicine in mRCC patients.

In our study, we observed a linear correlation of portal venous phase pretreatment mean CECT density with PFS and OS [HR = 0.956 ($P = .002$) and HR = 0.968 ($P = .001$), respectively; Table 2, Figure 2, *A* and *B*]. A very similar HR value was described by Han et al. in a comparison of the pretreatment mean CECT tumor density in the arterial phase and PFS [11]. We therefore conclude that the portal venous phase, which is less prone to timing artifacts and hemodynamic biases, is of similar predictive value of disease outcome in mRCC patients as the arterial phase. In contrast to the arterial phase, which is primarily indicative the vascularity of the tumor, the portal venous phase additionally represents the cellularity of the neoplastic lesion [28]. Dense tumors on CECT are more cellular and therefore necessitate a higher vascularization to grow, which renders them more prone to antiangiogenic treatment [29].

Furthermore, our study demonstrated a positive correlation of the portal venous phase pretreatment mean CECT tumor density and tumor growth at first follow-up ($P = .010$, Figure 2*C*), which demonstrates the strong association of pretreatment mean CECT density with clinically used treatment response assessment criteria relying on changes in tumor size [e.g., (revised) Choi or RECIST

criteria] [23]. A similar association between pretreatment mean CECT density and tumor growth was described for the arterial phase by Han et al. [11]. To the best of our knowledge, our study is the first to show that portal venous CECT is of similar predictive value for the clinical outcome in sunitinib-treated mRCC patients as arterial phase imaging, and we believe that the higher robustness of portal venous phase imaging strengthens the predictive value of assessing mean CECT tumor density on the outcome of sunitinib therapy.

In accordance with the study by Han et al. [11], we grouped the patients based on a PFS cut-off of 250 days. A ROC analysis yielded a ROC area under the curve of 0.722 (P = .003, Figure 3*A*) which corresponds well to the value reported by Han et al. [11]. Based on Youden's index, two optimal cut-offs with high sensitivity and specificity were determined: the first cut-off (63.67 HU) showed a similarly high sensitivity and specificity (70.4% and 69.4%, respectively). The second cut-off (68.67 HU) showed a very high specificity and a good sensitivity (80.6% and 59.3%, respectively), which underline its usefulness for identifying patients with lower long-term benefits from sunitinib treatment. In contrast to Han et al., where four subgroups were created based on somewhat arbitrarily chosen cut-off values [11], we decided to use a statistical method (Youden's J statistic) to determine the optimal cut-off values and created only two subgroups per cut-off value to facilitate clinical application and validation. The subpopulations of both cut-off values showed significant differences in PFS and OS ($P < .001$; Figure 3, *B-E*). A Kaplan-Meier survival analysis yielded significantly different survival curves for both PFS and OS (Figure 4, *A-D*), which underlines the utility of these cut-off values in distinguishing patients based on their probability of responding to treatment. We therefore derived two pretreatment mean CECT density cut-off values with high specificity and sensitivity associated with significant differences in patient PFS and OS. These cut-off values provide valuable basis for a more in-depth clinical validation.

Admittedly, our study had several limitations. Apart from its retrospective design, the exclusion of 47% (55 of 118) may incur a bias. Many patients who have not completed two treatment cycles due to adverse reactions were excluded from this study to ensure that our study investigates the efficacy of the sunitinib treatment in a standardized fashion. Furthermore, patients with inadequate scans and image quality had to be excluded as well. Moreover, certain at-risk patient populations (e.g., renally insufficient patients) cannot undergo CECT, and therefore, CECT attenuation measurements cannot be performed on these subjects. In addition, portal venous phase attenuation measurements are susceptible to changes in scan parameters and interindividual differences in cardiovascular dynamics (e.g., cardiac frequency and output). However, all included scans followed the standardized CT imaging protocol used at our institution. Moreover, methods yielding more direct measurements of tumor vascularity (e.g., perfusion CT) necessitate changes in imaging protocols and complex data analysis which may be difficult to implement in routine clinical practice. Furthermore, the proposed cut-off values may not be applicable in the context of a different contrast agent dose. Future studies should aim at clarifying the impact of potentially confounding factors such as cardiovascular parameters and the contrast agent dose on contrast enhancement in the lesions. Eventually, there was a slight variability in the timing of the baseline CT scan (up to 4 weeks before treatment) and the first response CT scan which was not avoidable due to the retrospective design of the study.

In summary, our study showed that higher pretreatment portal venous phase mean CECT tumor density was associated with prolonged PFS and OS (P = .002 and P = .001, respectively) in mRCC patients undergoing sunitinib treatment and that high mean CECT tumor density was associated with reduced tumor growth after two treatment cycles (P = .010). Two optimal CECT tumor density cut-off values with high specificity and sensitivity were established which identified subpopulations with significantly different OS and PFS ($P < .001$). The pretreatment mean CECT tumor density is therefore a highly promising predictive and prognostic factor for the treatment response of mRCC patients undergoing sunitinib therapy. These findings support the use of this relatively simple measurement to stratify treatment in mRCC patients, which represents a step toward personalized medicine in this patient population.

Funding information

This research did not receive any specific grant from funding agencies in the public, commercial, or not-for-profit sectors.

Acknowledgements

We thank the professional biostatistician (Nicole Graf, graf biostatistics, www.biostatistics.ch/) for her support in the statistical analysis of the data.

References

[1] Ferlay J, Soerjomataram I, Dikshit R, Eser S, Mathers C, Rebelo M, Parkin DM, Forman D, and Bray F (2015). Cancer incidence and mortality worldwide: sources, methods and major patterns in GLOBOCAN 2012. *Int J Cancer* **136**, E359-386.

[2] Sun M, Thuret R, Abdollah F, Lughezzani G, Schmitges. J, Tian Z, Shariat SF, Montorsi F, Patard JJ, Perrotte P, et al (2011). Age-adjusted incidence, mortality, and survival rates of stage-specific renal cell carcinoma in North America: a trend analysis. *Eur Urol* **59**, 135–141.

[3] Escudier B, Porta C, Schmidinger M, Algaba F, Patard JJ, Khoo V, Eisen T, and Horwich A, ESMO Guidelines Working Group (2014). Renal cell carcinoma: ESMO clinical practice guidelines for diagnosis, treatment and follow-up. *Ann Oncol* **25**, iii49–iii56.

[4] Oosterwijk-Wakka JC, de Weijert MCA, Franssen GM, Leenders WP, van der Laak JA, Boerman OC, Mulders PF, and Oosterwijk E (2015). Successful combination of sunitinib and girentuximab in two renal cell carcinoma animal models: a rationale for combination treatment of patients with advanced RCC. *Neoplasia* **17**, 215–224.

[5] Motzer RJ, Hutson TE, Tomczak P, Michaelson MD, Bukowski RM, Rixe O, Oudard S, Negrier S, Szczylik C, Kim ST, et al (2007). Sunitinib versus interferon alfa in metastatic renal-cell carcinoma. *N Engl J Med* **356**, 115–124.

[6] Cella D, Li JZ, Cappelleri JC, Bushmakin A, Charbonneau C, Kim ST, Chen I, and Motzer RJ (2008). Quality of life in patients with metastatic renal cell carcinoma treated with sunitinib or interferon alfa: results from a phase III randomized trial. *J Clin Oncol* **26**, 3763–3769.

[7] Gámez-Pozo A, Antón-Aparicio LM, Bayona C, Borrega P, Gallegos Sancho MI, García-Domínguez R, de Portugal T, Ramos-Vázquez M, Pérez-Carrión R, Bolós MV, Madero R, Sánchez-Navarro I, Fresno Vara JA, et al (2012). MicroRNA expression profiling of peripheral blood samples predicts resistance to first-line sunitinib in advanced renal cell carcinoma patients. *Neoplasia* **14**, 1144–1152.

[8] Han KS, Raven PA, Frees S, Gust K, Fazli L, Ettinger S, Hong SJ, Kollmannsberger C, Gleave ME, and So AI (2015). Cellular adaptation to VEGF-targeted antiangiogenic therapy induces evasive resistance by overproduction of alternative endothelial cell growth factors in renal cell carcinoma. *Neoplasia* **17**, 805–816.

[9] Goh V, Ganeshan B, Nathan P, Juttla JK, Vinayan A, and Miles KA (2011). Assessment of response to tyrosine kinase inhibitors in metastatic renal cell cancer: CT texture as a predictive biomarker. *Radiology* **261**, 165–171.

[10] Schmidt N, Hess V, Zumbrunn T, Rothermundt C, Bongartz G, and Potthast S (2013). Choi response criteria for prediction of survival in patients with

metastatic renal cell carcinoma treated with anti-angiogenic therapies. *Eur Radiol* **23**, 632–639.

[11] Han KS, Jung DC, Choi HJ, Jeong MS, Cho KS, Joung JY, Seo HK, Lee KH, and Chung J (2010). Pretreatment assessment of tumor enhancement on contrast-enhanced computed tomography as a potential predictor of treatment outcome in metastatic renal cell carcinoma patients receiving antiangiogenic therapy. *Cancer* **116**, 2332–2342.

[12] Nathan PD, Vinayan A, Stott D, Juttla J, and Goh V (2010). CT response assessment combining reduction in both size and arterial phase density correlates with time to progression in metastatic renal cancer patients treated with targeted therapies. *Cancer Biol Ther* **9**, 15–19.

[13] Smith AD, Shah SN, Rini BI, Lieber ML, and Remer EM (2013). Utilizing pre-therapy clinical schema and initial CT changes to predict progression-free survival in patients with metastatic renal cell carcinoma on VEGF-targeted therapy: a preliminary analysis. *Urol Oncol* **31**, 1283–1291.

[14] Mains JR, Donskov F, Pedersen EM, Madsen HHT, and Rasmussen F (2014). Dynamic contrast-enhanced computed tomography as a potential biomarker in patients with metastatic renal cell carcinoma: preliminary results from the Danish Renal Cancer Group Study-1. *Investig Radiol* **49**, 601–607.

[15] Koh D-M (2014). Science to practice: can intravoxel incoherent motion diffusion-weighted MR imaging be used to assess tumor response to antivascular drugs? *Radiology* **272**, 307–308.

[16] Messiou C, Orton M, Ang JE, Collins DJ, Morgan VA, Mears D, Castellano I, Papadatos-Pastos D, Brunetto A, Tunariu N, Mann H, Tessier J, Young H, et al (2012). Advanced solid tumors treated with cediranib: comparison of dynamic contrast-enhanced MR imaging and CT as markers of vascular activity. *Radiology* **265**, 426–436.

[17] Williams R, Hudson JM, Lloyd BA, Sureshkumar AR, Lueck G, Milot L, Atri M, Bjarnason GA, and Burns PN (2011). Dynamic microbubble contrast-enhanced US to measure tumor response to targeted therapy: a proposed clinical protocol with results from renal cell carcinoma patients receiving antiangiogenic therapy. *Radiology* **260**, 581–590.

[18] Hellbach K, Sterzik A, Sommer W, Karpitschka M, Hummel N, Casuscelli J, Ingrisch M, Schlemmer M, Graser A, and Staehler M (2016). Dual energy CT allows for improved characterization of response to antiangiogenic treatment in patients with metastatic renal cell cancer. *Eur Radiol*. http://dx.doi.org/10.1007/s00330-016-4597-7.

[19] Lassau N, Chami L, Benatsou B, Peronneau P, and Roche A (2007). Dynamic contrast-enhanced ultrasonography (DCE-US) with quantification of tumor perfusion: a new diagnostic tool to evaluate the early effects of antiangiogenic treatment. *Eur Radiol Suppl* **17**, 89–98.

[20] Lamuraglia M, Raslan S, Elaidi R, Oudard S, Escudier B, Slimane K, Penna RR, Wagner M, and Lucidarme O (2016). mTOR-inhibitor treatment of metastatic renal cell carcinoma: contribution of Choi and modified Choi criteria assessed in 2D or 3D to evaluate tumor response. *Eur Radiol* **26**, 278–285.

[21] Jamshidi N, Jonasch E, Zapala M, Korn RL, Brooks JD, Ljungberg B, and Kuo MD (2016). The radiogenomic risk score stratifies outcomes in a renal cell cancer phase 2 clinical trial. *Eur Radiol* **26**, 2798–2807.

[22] Oliver JH, Baron RL, Federle MP, and Rockette HE (1996). Detecting hepatocellular carcinoma: value of unenhanced or arterial phase CT imaging or both used in conjunction with conventional portal venous phase contrast-enhanced CT imaging. *Am J Roentgenol* **167**, 71–77.

[23] Thian Y, Gutzeit A, Koh D-M, Fisher R, Lote H, Larkin J, and Sohaib A (2014). Revised Choi imaging criteria correlate with clinical outcomes in patients with metastatic renal cell carcinoma treated with sunitinib. *Radiology* **273**, 452–461.

[24] Smith AD, Lieber ML, and Shah SN (2010). Assessing tumor response and detecting recurrence in metastatic renal cell carcinoma on targeted therapy: importance of size and attenuation on contrast-enhanced CT. *Am J Roentgenol* **194**, 157–165.

[25] van der Veldt AAM, Meijerink MR, van den Eertwegh AJM, Haanen JBAG, and Boven E (2010). Choi response criteria for early prediction of clinical outcome in patients with metastatic renal cell cancer treated with sunitinib. *Br J Cancer* **102**, 803–809.

[26] Smith AD, Shah SN, Rini BI, Lieber ML, and Remer EM (2010). Morphology, attenuation, size, and structure (MASS) criteria: assessing response and predicting clinical outcome in metastatic renal cell carcinoma on antiangiogenic targeted therapy. *Am J Roentgenol* **194**, 1470–1478.

[27] Eisenhauer EA, Therasse P, Bogaerts J, Schwartz LH, Sargent D, Ford R, Dancey J, Arbuck S, Gwyther S, Mooney M, et al (2009). New response evaluation criteria in solid tumours: revised RECIST guideline (version 1.1). *Eur J Cancer* **45**, 228–247.

[28] Monzawa S, Ichikawa T, Nakajima H, Kitanaka Y, Omata K, and Araki T (2007). Dynamic CT for detecting small hepatocellular carcinoma: usefulness of delayed phase imaging. *Am J Roentgenol* **188**, 147–153.

[29] Jain RK (2005). Normalization of tumor vasculature: an emerging concept in antiangiogenic therapy. *Science* **307**, 58.